sdg Interacting boson model : two nucleon transfer

Y D Devi and V K B Kota

Physical Research Laboratory,
Ahmedabad-380 009, India

Abstract : A brief overview of the *sdg* interacting boson model (*sdg* IBM) is given The two examples : (i) spectroscopic properties (spectra, $B(E2)$'s, $B(E4)$'s etc) of the rotor-γ unstable transitional Os-Pt isotopes and (ii) the analytical formulation of two nucleon transfer spectroscopic factors and sum-rule quantities are described in detail They demonstrate that *sdg* IBM can be employed for systematic description of spectroscopic properties of nuclei and that large number of analytical formulas, which facilitate rapid analysis of data and provide a clear insight into the underlying structures, can be derived using sdgIBM dynamical symmetries respectively

Keywords : Nuclear structure, interacting boson model

PACS No. : 21.10 –k

1. Introduction

In the past few years considerable amount of experimental data on $E4$ matrix elements, strength distributions and other observables that involve hexadecupole degree of freedom in nuclei has started accumulating and their theoretical understanding (using models or microscopic theories) is a challenging problem. This together with the microscopic theories of interacting boson model (IBM; which includes $l = 0$ (*s*-boson representing the pairing degree of freedom) and $l = 2$ (*d*-boson representing the quadrupole degree of freedom) bosons) and several other indirect signatures indicating that $l = 4$ (*g*-boson representing the hexadecupole degree of freedom) bosons should be included in IBM, lead to the development of the extended *sdg* interacting boson model (*sdg* IBM or simply *g*IBM). The *sdg* IBM is the only plausible model that allows one to systematically analyze hexadecupole data and understand the role of hexadecupole degree of freedom in nuclei (Devi and Kota 1992a).

Section 2 gives a brief overview of the various aspects of *sdg* IBM including data analysis. The two specific examples of *sdg* IBM studies : (i) systematic analysis of

spectroscopic properties of Pt-Os isotopes; (ii) the analytical formulation of two nucleon transfer spectroscopic factors and sum-rule quantities are described in detail in Sections 3 and 4 respectively. Finally Section 4 gives some concluding remarks.
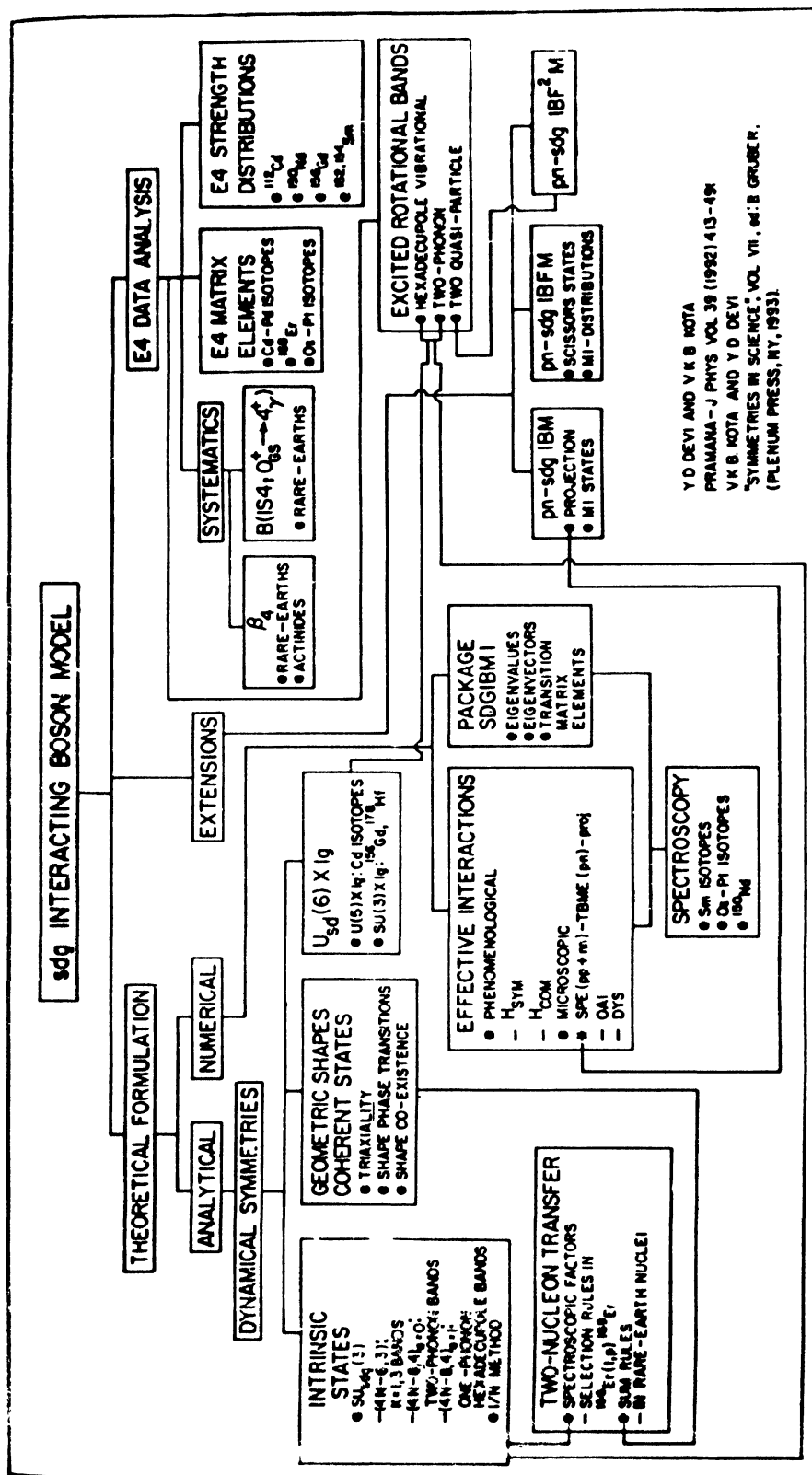
2. *sdg* IBM

In order to explore, understand and apply the *sdg* interacting boson model which is ideally suited for the study of hexadecupole properties of atomic nuclei, we carried out large number of studies by exploiting the dynamical symmetries (analytical in nature) and their interpolations (numerical in nature) and it is established with good number of examples that *sdg* IBM is a viable and powerful tool for systematically analyzing *E*4 properties of nuclei. These studies and the contributions by various other research groups, to the development of this model are reviewed recently (Devi and Kota 1992a, Kota and Devi 1993). A schematic outline of all these studies is given in Figure 1. In this article no attempt is made to describe all the developments in *sdg* IBM as complete details are given emphasizing the *sdg* IBM analysis of hexadecupole observables in (Devi and Kota 1992a) and dynamical symmetry aspects of the *sdg* IBM in (Kota and Devi 1993). In the following two sections two specific studies are described in some detail, one emphasizing the numerical aspects and the other emphasizing the analytical aspects of *sdg* IBM.

3. Spectroscopy of Pt-Os isotopes

Our purpose here is to show that a simple hamiltonian H_{SYM} (with 6–8 free parameters) defined in terms of Casimir operators of *g*IBM dynamical symmetries and a truncated space with no more than *g*-bosons (the resulting hamiltonian matrix dimensions being ~ 100) describes the spectroscopic properties of a chain of isotopes. To this end we choose the rotor-γ unstable transitional Pt=Os isotopes : ^{198}Pt, ^{196}Pt ^{194}Pt and ^{192}Os. For these isotopes, recently the *E*4 matrix elements for the decay of the first few 4$^+$levels to the ground state (GS) are deduced from the inelastic scattering of polarized protons $(\bar{p}, p')$ (Todd Baker *et al* 1989; Sethi *et al* 1990, 1991). The failure of attempts to describe this data within *sd*IBM and *sd*IBM $\oplus$ 1 *g* models lead to the present study with two *g*-bosons.

A simple hamiltonian H_{SYM} interpolating sdgIBM dynamical symmetries and *E*2 and *E*4 transition operators interpolating the group generators are employed in the calculations. The H_{SYM} is

$$H_{SYN} = \varepsilon_d \hat{n}_d + \varepsilon_g \hat{n}_g + \alpha_1 \Big[H(SU_{sdg}(3))\Big] + \alpha_2 \Big[H(SU_{sdg}(5))\Big]$$

$$+ \alpha_3 \Big[H(SU_{sdg}(6))\Big] + \alpha_4 \Big[H(O_{sdg}(15))\Big] + \alpha_5 \Big[H(O_{sd}(6))\Big]$$

$$+ \alpha_6 [H(O(3))] \, H(SU_{sdg}(3)) = -\frac{3}{4} \, Q^2(s).Q^2(s)$$

Figure 1. Schematic overview of various developments in sdgIBM

$$Q_\mu^2(s) = 4\sqrt{\frac{7}{15}}\left(s^\dagger\tilde{d}+d^\dagger\tilde{s}\right)_\mu^2 - 11\sqrt{\frac{2}{21}}\left(d^\dagger\tilde{d}\right)_\mu^2 + \frac{36}{\sqrt{105}}\left(d^\dagger\tilde{g}+g^\dagger\tilde{d}\right)_\mu^2$$

$$- 2\sqrt{\frac{33}{7}}\left(g^\dagger\tilde{g}\right)_\mu^2; \quad H(SU_{sdg}(5)) = -4\left\{G^2.G^2+G^4.G^4\right\};$$

$$G_\mu^2 = \frac{1}{\sqrt{5}}(\left(s^\dagger\tilde{d}+d^\dagger\tilde{s}\right)_\mu^2 - \sqrt{\frac{3}{14}}\left(d^\dagger\tilde{d}\right)_\mu^2 + \frac{6}{\sqrt{245}}\left(d^\dagger\tilde{g}+g^\dagger\tilde{d}\right)_\mu^2$$

$$+ \frac{\sqrt{198}}{14}\left(g^\dagger\tilde{g}\right)_\mu^2 \quad G_\mu^4 = \frac{1}{\sqrt{5}}(\left(s^\dagger\tilde{g}+g^\dagger\tilde{s}\right)_\mu^4 + \frac{2}{7}\left(d^\dagger\tilde{d}\right)_\mu^4$$

$$+ \sqrt{\frac{55}{98}}\left(d^\dagger\tilde{g}+g^\dagger\tilde{d}\right)_\mu^4 + \sqrt{\frac{143}{980}}\left(g^\dagger\tilde{g}\right)_\mu^4; \quad H(SU_{sdg}(6))$$

$$= -4\left\{h^2.h^2 + h^4.h^4\right\};$$

$$h_\mu^2 = -\frac{1}{\sqrt{6}}\left(s^\dagger\tilde{d}+d^\dagger\tilde{s}\right)_\mu^2 + \frac{5}{7\sqrt{6}}\left(d^\dagger\tilde{d}\right)_\mu^2 - \frac{9}{14\sqrt{2}}\left(d^\dagger\tilde{g}+g^\dagger\tilde{d}\right)_\mu^2$$

$$- \frac{\sqrt{33}}{14}\left(g^\dagger\tilde{g}\right)_\mu^2$$

$$h_\mu^4 = -\frac{1}{\sqrt{6}}\left(s^\dagger\tilde{g}+g^\dagger\tilde{s}\right)_\mu^4 - \frac{3}{14}\sqrt{\frac{5}{2}}\left(d^\dagger\tilde{d}\right)_\mu^4 - \frac{1}{14}\sqrt{\frac{55}{3}}\left(d^\dagger\tilde{g}+g^\dagger\tilde{d}\right)_\mu^4$$

$$+ \frac{1}{14}\sqrt{\frac{143}{2}}\left(g^\dagger\tilde{g}\right)_\mu^4;$$

$$H(O_{sdg}(15)) = I^2 \cdot I^2 + I^4 . I^4; \quad I_\mu^2 = \left(s^\dagger\tilde{d}+d^\dagger\tilde{s}\right)_\mu^2, \quad I_\mu^4 = \left(s^\dagger\tilde{g}+g^\dagger\tilde{s}\right)_\mu^4;$$

$$H(O_{sd}(6)) = I^2 . I^2$$

$$H(O(3)) = \mathbf{L}.\mathbf{L}; \quad \mathbf{L}_\mu^1 = \sqrt{10}\left\{\left(d^\dagger\tilde{d}\right)_\mu^1 + \sqrt{6}\left(g^\dagger\tilde{g}\right)_\mu^1\right\} \qquad (1)$$

In (1) $\{Q^2(s)\}$, $\{G^2, G^4\}$, $\{h^2, h^4\}$ and $\{I^2, I^4\}$ are generators of $SU_{sdg}(3)$, $SU_{sdg}(5)$, $SU_{sdg}(6)$ and $O_{sdg}(15)$ respectively (I^2 is also a generator of $O_{sd}(6)$). The $E2$ and $E4$ transition operators are chosen keeping in mind that $SU_{sdg}(3)$ and $O_{sdg}(15)$ symmetries are relevent for the nuclei in Os–Pt region. In terms of $SU_{sdg}(3)$ quadrupole generator $Q_\mu^2(s)$ and the $O_{sdg}(15)$ (or $O_{sd}(6)$) quardrupole generator I_μ^2 of eq. (1), the $E2$ operator is $T^{E2} = \alpha[Q_\mu^2(s)+\beta I_\mu^2]$. Similarly the $E4$ transition operator is chosen to be a linear combination on the Q_{osc}^4.

$$Q^4_{osc.\mu} = \left[\left(s^\dagger \tilde{g} + g^\dagger \tilde{s} \right)^4_\mu + \frac{19\sqrt{5}}{28} \left(d^\dagger \tilde{d} \right)^4_\mu - \frac{5\sqrt{11}}{14} \left(d^\dagger \tilde{g} + g^\dagger \tilde{d} \right)^4_\mu \right.$$

$$\left. + \frac{3\sqrt{143}}{28} \left(g^\dagger \tilde{g} \right)^4_\mu \right] \tag{2}$$

and the $O_{sdg}(15)$ rank-4 generator I^4_μ defined in (1), $T^{E4} = \xi \left[I^4_\mu + \eta Q^4_{osc.\mu} \right]$. It should be noted that although Q^4_{osc} is not a generator of any of the gIBM dynamical symmetries, it can be viewed as a close analogue of $Q^2(s)$ but of rank-4, as the factors multyplying the terms in the Q^4_{osc} are obtained by evaluating the matrix elements of $r^4 Y^4$ operator in the sdg harmonic oscillator basis and it is successfully used in earlier studies describing data relating to $E4$ observables (Devi and Kota 1992b).

With the transition operators given in (2) and (3), $B(E2)$ values,

$$B(E2 ; L_i \rightarrow L_f) = \frac{\left| < L_f \| T^{E2} \| L_i > \right|^2}{(2L_i + 1)}$$

and the absolute $E2$ and $E4$ reduced matrix elements

$$M(E\lambda ; L_i \rightarrow L_f) = \left| < L_f \| T^{E\lambda} \| L_i \right| \quad ; \lambda = 2, 4$$

are calculated and compared with data.

The boson number $N = 5, 6, 7$ and 8 for ^{198}Pt, ^{196}Pt, ^{194}Pt and ^{192}Os and based on occupation numbers one sees that one can safely use a truncated space $n_s \geq 1, 2, 2$ and 2 respectively. The successful calculations for Sm isotopes (Devi and Kota 1992b) lead to the restriction $n_g \leq 2$. With these truncations (the maximum hamiltonian matrix dimensions being 27, 27, 53 and 95 respectively) and with the parameters given in Table 1. The spectra

Table 1. Parameters employed in the sdgIBM calculations

Nucleus	ε_d (Mev)	ε_g (MeV)	α_1 (keV)	α_2 (keV)	α_3 (keV)	α_4 (keV)	α_5 (keV)	α_6 (keV)	α (eb)	β	ζ (eb^2)	η
^{198}Pt	0 49	0.75	1.35	0	1 98	28.3	-53.4	16	0 03	10/3	0.09	$-2/3$
^{196}Pt	0 32	0.65	-1.26	0	62.5	45 1	-55 4	13	0 03	3	0 043	8/23
^{194}PT	0.04	0.40	0.75	0	0	-13.2	-23.7	15	0 052	0	0.27	0
^{192}Os	0.23	0,62	0.36	6.2	0	-2.2	-7.2	10	0.12	$-3/2$	0.0143	$-10/3$

for the above four nuclei are calculated (gIBM (2 g)) and they are compared with data and other sdg IBM calculations ($sd \times 1$ g due to Sethi *et al* (1991) and Todd Baker *et al* (1985) and gIBM (full), where there is no truncation of the space, is due to Kuyucak *et al* (1991) in Figures 2a–d. The experimental data for ^{198}Pt is due to Sethi *et al* (1990) and from NDS (1983a), for ^{196}Pt is due to Sethi *et al* (1991), Bolotin *et al* (1981) and from NDS (1979), for

[194]Pt is due to Sethi *et al* (1990) and from NDS (1989) and for [192]Os is from NDS (1983b). The numbers given in the parenthesis to the extreme left in Figures 2a–d are the *g*-boson
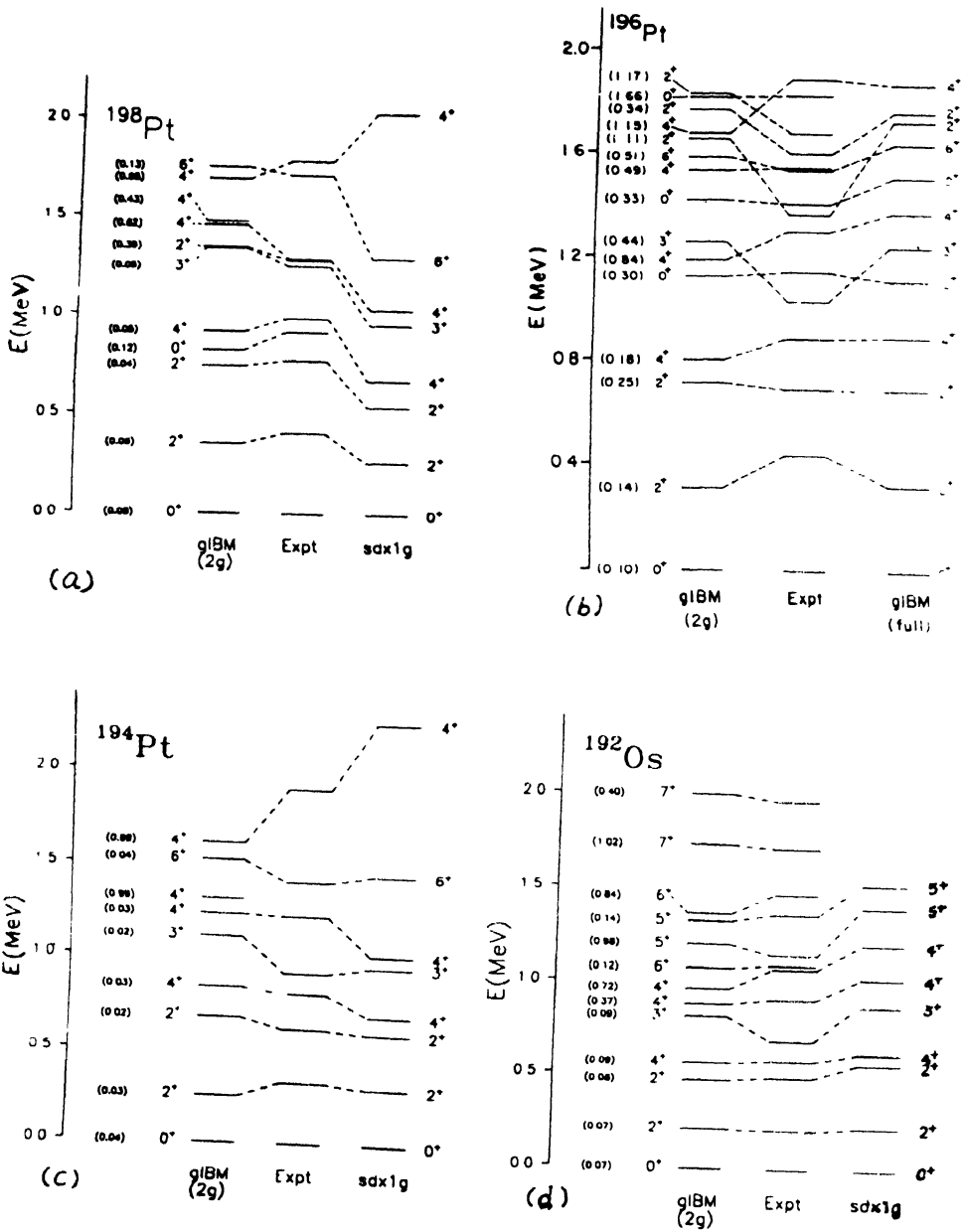

Figure 2. Experimental and calculated (sdgIBM) spectra for Os–pt isotopes.

occupation numbers and from them one can infer the hexadecupole content in the wavefunctions. It is seen from the figures that the quality of agreements in the *sdg* IBM (2*g*) calculations is much better than in *sd* × 1*g* and as good as *g*IBM (full) results. The quality

of agreements extends to $E2$ and $E4$ transition matrix elements; the results are given in Tables 2a–d and Table 3 respectively. Thus the consistently good description of spectra,

Table 2a. B(E2) values for ^{198}Pt.

$L_i \rightarrow L_f$	$B(E2 ; L_i \rightarrow L_f) (e^2b^2)$		
	Expt[a]	gIBM[b] (2g)	sdIBM[c]
$2_1^+ \rightarrow 0_1^+$	0.204 ± 0.02	0.280	0 194
	0 222 ± 0.001		
$2_2^+ \rightarrow 2_1^+$	0.185 ± 0.024	0 257	0 134
	0 262 ± 0.038		
	0 255 ± 0 048		
$2_2^+ \rightarrow 0_1^+$	$(3 ± 1) \times 10^{-4}$	10^{-3}	10^{-4}
$0_2^+ \rightarrow 2_1^+$	0.191 ± 0.051	0 061	0 017
	0 179 ± 0.048		
$4_1^+ \rightarrow 2_1^+$	0 27 ± 0.023	0 379	0 253
	0 262 ± 0.028		
$2_3^+ \rightarrow 2_2^+$	0.015 ± 0.010	0 018	10^{-4}
$2_3^+ \rightarrow 2_1^+$	0 004 ± 0 003	10^{-4}	5×10^{-4}
$2_3^+ \rightarrow 0_1^+$	$(4 ± 3) \times 10^{-4}$	5×10^{-4}	~ 0
$6_1^+ \rightarrow 4_1^+$	≥ 0.395	0 358	0.240

[a] NDS (1990), Bolotin *et al* (1981)
[b] Present calculation
[c] Bolotin *et al* (1981)

Table 2b. B(E2) values for ^{196}Pt

$L_i \rightarrow L_f$	$B(E2 , L_i \rightarrow L_f) (e^2b^2)$			
	Expt[a]	gIBM		
		$(1g)$[a]	$(2g)$[b]	$(3g)$[c]
$2_1^+ \rightarrow 0_1^+$	0.344 ± 0.01	0.315	0 320	0.294
	0.276			
	0.288 ± 0.014			
	0.30			
$2_2^+ \rightarrow 0_1^+$	3×10^{-6}	0.002	0 002	0 007
$2_2^+ \rightarrow 2_1^+$	0.35 ± 0.031	0.391	0 177	0.283
	0.26 ± 0.055			
$4_1^+ \rightarrow 2_1^+$	0.043 ± 0.032	0.443	0.437	0 415
	0.443 ± 0.026			
	0.380 ± 0.030			
$0_2^+ \rightarrow 2_1^+$	0.033 ± 0.007	0.006	0.020	0.075
	0.021 ± 0.01			

Table 2b. *(Cont'd.)*

$L_i \to L_f$	$B(E2 ; L_i \to L_f)$ (e^2b^2)			
	Expt[a]	gIBM		
		$(1g)$[a]	$(2g)$[b]	$(3g)$[c]
$0_2^+ \to 2_2^+$	0.142 ± 0.077	0.448	0.299	0.177
$4_2^+ \to 2_1^+$	0.003	0.003	0.013	0.002
	0.0023 ± 0.0008			
$4_2^+ \to 2_2^+$	0.177 ± 0.035	0.246	0.068	0.199
	0.218 ± 0.043			
$4_1^+ \to 3_1^+$	≤ 0.06	0.026	0.020	- - -
$4_2^+ \to 4_1^+$	0.193 ± 0.097	0.20	0.084	0.14
	0.218 ± 0.054			
	0.180 ± 0.090			
$6_1^+ \to 4_1^+$	0.421 ± 0.116	0.50	0.359	0.450
	0.494 ± 0.370			
	0.400 ± 0.110			

[a] Sethi *et al* (1991). Devi and Kota (1992a)
[b] Present calculation
[c] Navratil and Dobes (1991)

Table 2c. B(E2) values for ^{194}Pt

$L_i \to L_f$	$B(E2 ; L_i \to L_f)$ (e^2b^2)		
	Expt[a]	gIBM[b] $(2g)$	pnIBM[c]
$2_1^+ \to 0_1^+$	0.374 ± 0.016	0.341	0.357
	0.324 ± 0.003		
$4_1^+ \to 2_1^+$	0.47 ± 0.03	0.478	0.496
	0.449 ± 0.022		
$6_1^+ \to 4_1^+$	0.32 ± 0.08	0.492	0.544
	0.48 ± 0.14		
$4_2^+ \to 2_2^+$	0.28 ± 0.12	0.193	0.275
	0.18 ± 0.06		
	0.69 ± 0.39		
$2_2^+ \to 0_1^+$	0.0014 ± 0.0002	0.009	3×10^{-5}
	0.0015 ± 0.0002		
$2_2^+ \to 2_1^+$	0.58 ± 0.07	0.295	0.517
	0.423 ± 0.015		
	0.60 ± 0.07		
$4_2^+ \to 4_1^+$	0.87 ± 0.43	0.130	0.276
$4_2^+ \to 2_1^+$	0.01 ± 0.005	0.007	0.004

[a] Baktash *et al* (1978), Stelzer *et al* (1977)
[b] Present calculation
[c] Bijker *et al* (1980)

Table 2d. $E2$ matrix elements in ^{192}Os.

$L_i \rightarrow L_f$	$|<J_f||T^{E2}||J_i>|$ (eb)		
	Expt[a]	gIBM	
		$(2g)$[b]	(full)[c]
$2_1^+ \rightarrow 0_1^+$	1.457 ± 0.018	1.594	1.457
$4_1^+ \rightarrow 2_1^+$	$2.115 \, (^{+0.038}_{-0.044})$	2 720	2.330
$6_1^+ \rightarrow 4_1^+$	$2.93 (^{+0.10}_{-0.08})$	3 430	2.960
$2_2^+ \rightarrow 2_1^+$	$1.224 (^{+0.030}_{-0.016})$	1.112	1.231
$2_2^+ \rightarrow 0_1^+$	$0.425 (^{+0.008}_{-0.014})$	0.405	0 289
$2_2^+ \rightarrow 4_1^+$	$0.35 (^{+0.12}_{-0.07})$	0.574	0 203
$0_2^+ \rightarrow 2_1^+$	$0.066 (^{+0.012}_{-0.013})$	0 643	0 152
$0_2^+ \rightarrow 2_2^+$	$0 449 (^{+0.044}_{-0 056})$	0 895	0 689
$4_2^+ \rightarrow 4_1^+$	$1.35 (^{+0.10}_{-0.08})$	1 074	1 327
$4_2^+ \rightarrow 2_2^+$	1.637 ± 0.050	1.579	1.562
$4_2^+ \rightarrow 2_1^+$	$0.125 (^{+0 018}_{-0 010})$	0.462	0.098
$4_2^+ \rightarrow 6_1^+$	$0.40 (^{+0 20}_{-0 18})$	0.797	0.298
$6_2^+ \rightarrow 6_1^+$	$1 49 (^{+0.30}_{-0 20})$	0.839	1.324
$6_2^+ \rightarrow 4_2^+$	$2.09 (^{+0 13}_{-0 17})$	1.873	2.270
$6_2^+ \rightarrow 4_1^+$	0.067 ± 0.076	0.060	0.262
$4_3^+ \rightarrow 4_2^+$	1.19 ± 0.22	0 792	0.583
$4_3^+ \rightarrow 3_1^+$	$1.63 (^{+0 20}_{-0 36})$	1.038	0.836
$4_3^+ \rightarrow 2_2^+$	$0.79 (^{+0 12}_{-0 14})$	0 502	0 694
$4_3^+ \rightarrow 2_1^+$	$0.113 (^{+0.064}_{-0.046})$	0.428	0.153

[a] Wu (1983)
[b] Present calculation
[c] Lac and Kuyucak (1992)

Table 3. Select $E4$ matrix elements in $^{194,196,198}Pt$ and ^{192}Os nuclei.

Nucleus	$E(4_f^+)$MeV	$L_i \rightarrow L_f$	$B(E4 ; L_i \rightarrow L_f)$ $(10^{-2}e^2b^2)$	
			Expt[a]	gIBM
^{198}Pt	0.985	$0_1^+ \rightarrow 4_1^+$	2.07 ± 0.09	2.16[b]
			0.81 ± 0.81	
	1.287	$0_1^+ \rightarrow 4_2^+$	1.54 ± 0.15	1.54[b]
			$.\ 0.04$	1.30[c]
	1.785	$0_1^+ \rightarrow 4_3^+$	0.88 ± 0.13	0.72[b]
				2.82[c]

Table 3. *(Cont'd)*

Nucleus	$E(4_f^+)$MeV	$L_i \to L_f$	$B(E4 : L_i \to L_f)$ $(10^{-2}e^2b^2)$ Expt[a]	gIBM
^{196}Pt	0 877	$0_1^+ \to 4_1^+$	3.06 ± 0.25	3.50[b]
			2 40 ± 0 50	3 40[d]
			3 24 ± 2.5	2 50[c]
	1 293	$0_1^+ \to 4_2^+$	2 47 ± 0.28	3 1[b]
			2 0 ± 0 40	0 80[d]
			< 1 96	1 99[c]
	1 537	$0_1^+ \to 4_3^+$	0 45 ± 0 08	0 92[b]
	1 887	$0_1^+ \to 4_4^+$	4 0 ± 0 2	1 99[b]
			4 4 ± 1 3	4 90[d]
				2 62[c]
^{194}Pt	0 811	$0_1^+ \to 4_1^+$	⌐.8 ± 0 27	4.22[b]
			3 65 ± 0 34	3 31[c]
			5 29 ± 3 7	
	1 229	$0_1^+ \to 4_2^+$	1.32 ± 0 16	1.79[b]
			1 72 ± 0 16	2 72[c]
			1 69 ± 0 78	,
	1 911	$0_1^+ \to 4_3^+$	5 24 ± 0 32	4 42[b]
			7.84 ± 0 56	1.93[c]
^{192}Os	0 58	$0_1^+ \to 4_1^+$	4 00	4 71[b]
			3 84 ± 0 43	
	0 91	$0_1^+ \to 4_2^+$	1 39	1 02[b]
			1 35 ± 0 67	
	1 07	$0_1^+ \to 4_3^+$	1.21	2.25[b]
			1 ι7	

[a] Todd Baker *et al* (1985, 1989), Sethi *et al* (1990, 1991)

[b] Present Calculation

[c] Kuyucak *et al* (1991)

[d] Navratil and Dobes (1991)

$E2$ and $E4$ properties with a $2g$-boson truncation establishes that the present truncation scheme is meaningful for Pt–Os isotopes.

4. Two nucleon transfer

Two nucleon transfer (TNT) cross sections and the corresponding spectroscopic factors (or strengths) are one of the most valuable observables in nuclear structure and they provide deeper insights into effects due to pairing degrees of freedom, single particle aspects *etc*. The IBM provides a natural frame work for a unified and analytical description of TNT strengths and cross sections. This analytical feature of IBM together with the rich dynamical symmetry structures in sdg IBM make TNT studies in sdg IBM an ideal probe to infer the structure of the excited rotational bands (two phonon quadrupole, one phonon

hexadecupole vibrational, two quasi particle) and also about shapes and shape phase transitions.

In sdgIBM the TNT operators for $l = 0, 2, 4$ transfers, ignoring cut-off factors (Devi and Kota 1991) that depend on boson numbers, are

$$
\begin{aligned}
P_+^{l=0} &= \eta +_0 s^\dagger & P_-^{l=0} &= \eta -_0 \tilde{s} \\
P_+^{l=2} &= \eta +_2 d^\dagger & P_-^{l=2} &= \eta -_2 \tilde{d} \\
P_+^{l=4} &= \eta +_4 g^\dagger & P_-^{l=4} &= \eta -_4 \tilde{g}
\end{aligned}
$$

where (+) is for particle addition and (−) is for particle removal and η's are free parameters. Employing these operators analytical expressions for TNT strengths

$$
S_l^{(\pm)}\left(N;0_{GS}^+ \rightarrow N \pm 1;L_f^+\right) = (\eta \pm l)^2 \left|\left\langle N \pm 1;L_f^+ \|P_{(\pm)}^l\| N;0_{GS}^+\right\rangle\right|^2 \delta_{l,f} \tag{3}
$$

in the $SU_{sdg}(3)$ limit are reported by Devi and Kota (1991) and for the $SU_{sd}(3) \times 1g$ limit the results are reported here.

In the $SU_{sdg}(3)$ limit as shown in Figure 3, in addition to the usual ground, beta and gamma bands generated by the $SU(3)$ irreducible representations (irreps) $(4N,0)K^\pi = 0$, $(4N-4, 2)K^\pi = 0$ and $(4N-4, 2)K^\pi = 2$ respectively, there are two new features : (i) odd K bands arising due to the irrep $(4N-6, 3)K^\pi = 1, 3$; (ii) two types of 4^+ (also 0^+ and 2^+ bands)

Figure 3. Analytical expressions for TNT strengths in the $SU_{sdg}(3)$ limit.

arising from the two $(4N-8, 4)$ irreps labeled $\alpha = 0, 1$. From the structure of the intrinsic states shown in the inset to Figure 3, the $\alpha = 0$ bands are two phonon in nature and the $\alpha =$

1 bands are one phonon hexadecupole in nature. The analytical expressions (functions of N the boson number) given in Figure 3 allow the rapid analysis of data and makes transparent the structure of rotational bands as the selection rule forbidding (indicated by dashed lines in the figure) the excitation of two phonon bands. In fact the branching/selection rules provided by these analytical expressions explain the observed TNT strengths in the ^{166}Er (t, p) ^{168}Er data; details of this data analysis are given ahead.

In the $SU_{sd}(3) \times 1$ g limit the coupling of a g-boson to the core described by the $SU_{sd}(3)$ limit gives rise to $K^\pi = 0, 1, 2, 3, 4$ bands in addition to the ground, beta and gamma bands generated by the $(2N, 0)$ $K^\pi = 0$, $(2N{-}4, 2)K^\pi = 0$ and $(2N{-}4, 2)K^\pi = 2$ irreps of $SU_{sd}(3)$ limit respectively and the two phonon quadrupole bands arising due to $(2N{-}8, 4)$ irrep with $K^\pi = 0, 2, 4$. The analytical expressions for TNT strengths are shown in Figure 4.
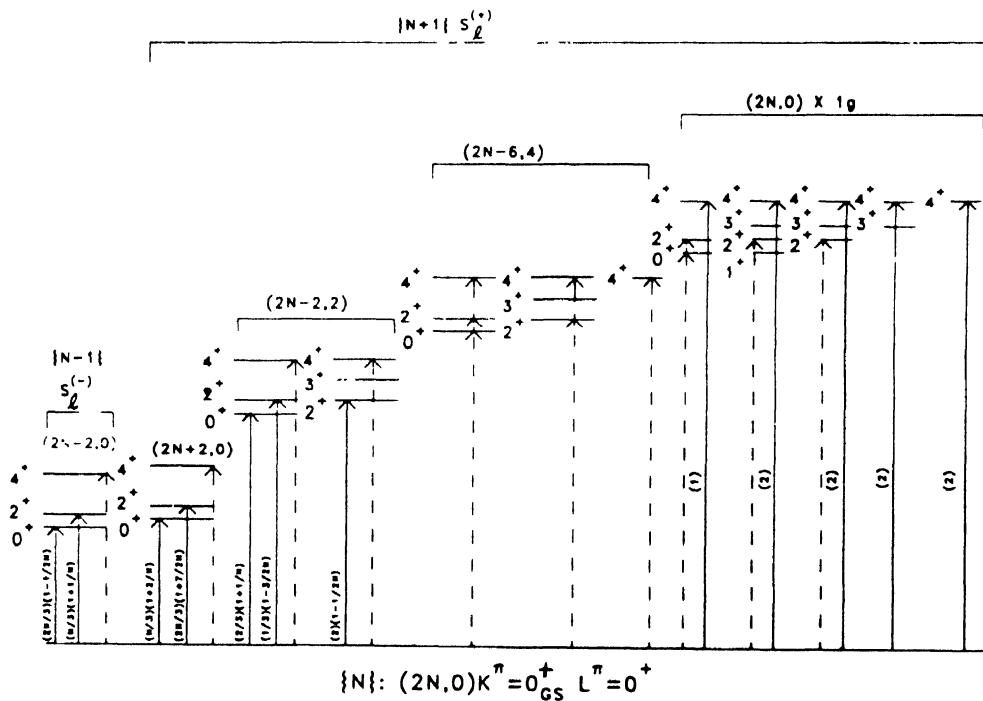

Figure 4. Analytical expressions for TNT strengths in the $SU_{sd}(3) \times 1$ g limit.

These results establish that TNT studies clearly determine the appropriateness of $SU_{sdg}(3)$ limit and the $SU_{sd}(3) \times 1$ g limit descriptions as in the example of ^{166}Er(t, p) ^{168}Er data described below;

- The strength to $IK^\pi = 44^+$ at 2.06 MeV is observed to be rather weak. In the $SU_{sdg}(3)$ limit this level belongs to $(4N{-}4, 4)_{\alpha=0}$ which is two-phonon in nature and the selection rule then explains the data. In the $SU_{sd}(3) \times 1$ g limit this level belongs to $(2N{-}6, 4)$ irrep as shown in Figure 4 which then also explains the selection rule.

- In $Su_{sd}(3)$ and $SU_{sd}(3) \times 1\ g$ limits $K^\pi = 0_3^+$, 0_4^+ and 2_2^+ cannot be excited. These forbidden levels are observed experimentally. The strengths to 0_1^+, 0_2^+ (1.217 MeV), 0_3^+ (1.422 MeV) and 0_4^+ (1.833 MeV) are (100, 15, 10, 2.4) and (100, 8.4, 15.2, 0) in experiment and $SU_{sdg}(3)$ limit respectively.

- The strength to $IK^\pi = 2\ 2_2^+$ is 6 times the strength to $2\ 2_1^+$ in $SU_{sdg}(3)$ limit and the data value is 5 ; $2\ 2_2^+$ belongs to $(4N-8, 4)_{\alpha=0}$. In the $SU_{sd}(3) \times 1\ g$ limit the value of this ratio is zero.

- The 4_5^+ (1.737 MeV) level is strongly populated in experiments. In $SU_{sdg}(3)$ limit this level belongs 4 3_1^+ and then single step excitation to this level is possible which then explains the data. This is a forbidden transition in the $SU_{sd}(3) \times 1\ g$ limit.

Thus TNT studies in $SU_{sd}(3) \times 1\ g$ and $SU_{sdg}(3)$ limits clearly establish that ^{168}Er is a good $SU_{sdg}(3)$ nucleus.

In general going beyond dynamical symmetries TNT studies can still have analytical formulation by considering the ratio $R_\pm$ (the advantage in dealing with this ratio is that it makes it a good approximation to deal with spectroscopic factors in place of cross sections) proposed by Grarrett *et al* (1990) which results in a sum-rule quantity in sdgIBM,

$$R_\pm = \frac{\sum\limits_{f \neq GS} S_{(l=0)}^{(\pm)} \left(N;\ 0_{GS}^+ \rightarrow N \pm 1;\ 0_f^+ \right)}{S_{(l=0)}^{(\pm)} \left(N;\ 0_{GS}^+ \rightarrow N \pm 1;\ 0_{GS}^+ \right)}$$

$$R_+ = \frac{1 + \left\langle N; \beta_2^0, \beta_4^0, \gamma^0 \left| s^\dagger s \right| N; \beta_2^0, \beta_4^0, \gamma^0 \right\rangle}{\left| \left\langle N+1; \beta_2^0, \beta_4^0, \gamma^0 \left| s^\dagger \right| N; \beta_2^0, \beta_4^0, \gamma^0 \right\rangle \right|^2} - 1$$

$$= \frac{\left(\beta_2^0 \right)^2 + \left(\beta_4^0 \right)^2}{N} + O(1/N^2) \qquad (4)$$

$$R_- = \frac{\left\langle N; \beta_2^0, \beta_4^0, \gamma^0 \left| s^\dagger s \right| N; \beta_2^0, \beta_4^0, \gamma^0 \right\rangle}{\left| \left\langle N-1; \beta_2^0, \beta_4^0, \gamma^0 \left| s \right| N; \beta_2^0, \beta_4^0, \gamma^0 \right\rangle \right|^2} - 1$$

$$= 0 \text{ in all cases} \qquad (5)$$

The equilibrium coherent states $\left| N; \beta_2^0, \beta_4^0, \gamma^0 \right\rangle$ are determined for all the dynamical symmetries of *sdg* IBM by Devi and Kota (1990). The analytical results in eqs. (4, 5) are used in analyzing the data (data is due to D.G.Burke; private communication) for the ratio R in rare-earth nuclei and the results are shown in Figure 5. Due to particle-hole symmetry in determining the boson number N, both the (t, p) data shown in the Figure 5 correspond to $R = R_+$. The analysis clearly brings out the regions of applicability of *sdg* dynamical symmetries (the ratio R is same for both $SU_{sdg}(3)$ and $SU_{sdg}(5)$ limits) and they are consistant with the conclusions drawn from coherent state studies (Devi and Kota 1990).

Although the average trend in data is well explained by symmetry limits, there are peaks observed (for example in the neutron number 90 region) and they correspond to shape-phase transitions. To describe the peaks a hamiltonian interpolating shperical-deformed
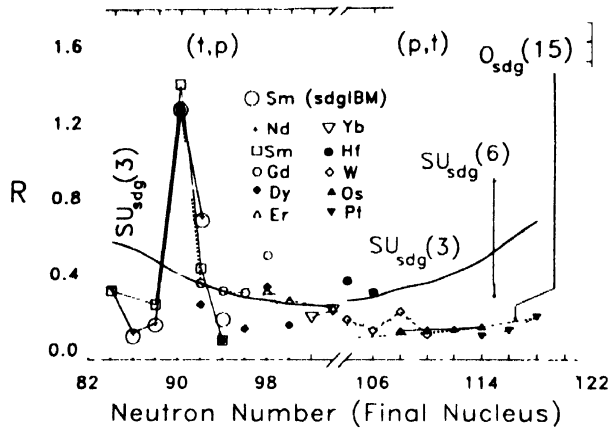

Figure 5. Experimental data for the ratio R in rare-earth nuclei and the corresponding sdgIBM results

shapes is employed in a detailed sdgIBM numerical calculations (Devi and Kota 1992b) and the peak is well described by the calculations (big circles in Figure 5). Thus the analysis of the ratio R gives information on the regions of relevance of sdgIBM dynamical symmetries ((*i.e.*) about shapes) and also about shape phase transitions.

5. Conclusions

The two specific examples : (i) the spectroscopy of a chain of isotopes (*i.e.*) the rotor-γ unstable transitional Pt-Os isotopes; (ii) the analytical formulation of two nucleon transfer strength in $SU_{sdg}(3)$, $SU_{sd}(3) \times 1$ g limits and the ratio R, demonstrate that sdgIBM is a powerful and viable tool in analyzing collective spectroscopic properties of heavy nuclei. In order to include the description of single particle aspects one has to extend sdgIBM to include a few (1–4) quasi particle excitations and this project is in progress (Devi and Kota 1993).

References

C Baktash *et al Phys. Rev.* **C18** 131 (1978)

R Bijker *et al Nucl. Phys.* **A344** 207 (1980)

Bolotin *et al Nucl. Phys* **A370** 146 (1981)

Y D Devi and V K B Kota Z *Phys.* **A337** 15 (1990)

Y D Devi and V K B Kota *J. Phys.* **G 17** L185 (1991)

Y D Devi and V K B Kota *Pramana-J. Phys.* **39** 413 (1992a)

Y D Devi and V K B Kota *Phys. Rev.* **C45** 2238 (1992b)

P E Garrett, D G Burke, Y D Devi and V K B Kota *Book of Abstracts* (Symposium in Honour of A Arima, Santa Fe, New Mexico) pp 57 (1990)

Y D Devi and V K B Kota *sdg Interacting Boson Model Quasi-particle Extensions,* to appear in the proceedings of the workshop on 'Nuclear Structure Physics', held at Puri (India), March 5-7 (1993); Physical Research Laboratory Report **PRL-TH/93-7** (1993)

V K B Kota and Y D Devi *in Symmetries in Science* **VII** (ed) B Gruber (New York Plenum) in press (1993)

S Kuyucak, V S Lac, I Morrison and B R Barrett *Phys. Lett.* **263B** 347 (1991)

V S Lac and S Kuyucak *Nucl Phys.* **539** 418 (1992)

P Navratil and J Dobes *Nucl. Phys* **A533** 223 (1991)

Nuclear Data Sheets **28** 485 (1979)

Nuclear Data Sheets **40** 301 (1983a)

Nuclear Data Sheets **40** 425 (1983b)

Nuclear Data Sheets **56** 75 (1989)

Nuclear Data Sheets **60** 527 (1990)

A Sethi *et al Nucl Phys* **A518** 536 (1990)

A Sethi *et al Phys. Rev* **C44** 700 (1991)

K Stelzer *et al Phys Lett* **70B** 297 (1977)

F Todd Baker *et al Nucl Phys* **A501** 546 (1989)

F Todd Baker *et al Phys Rev* **C32** 2212 (1985)

C Y Wu *PhD Thesis* (University of Rochester) (1983)

Note added in proof :

In Figure 4 $S_{(l)}^{(+)}\left(N;(2N,0)\ 0_{GS}^+ \to N+1;\ (2N-2,2)\ K_f = 0^+,\ L_f = 0_f^+\right)$ should be 2/3 but not (2/3) (1+1/N). The S_l^+ strengths shown in Figures 3, 4 satisfy some important sum rules. For example $\sum_{L_f} S_{(l)}^{(+)}\left(N;\ (\eta N,0)\ 0_{GS}^+ \to N+1;\ (\lambda_f \mu_f)K_f L_f\right)$ is $(2 - \delta_{K_f},0)$ for the ground and one phonon bands while it is zero for the two phonon bands; $\eta = 4$ for SU_{sdg} (3) and 2 for SU_{sd} (3) × 1 g. Note that the sum rule is independent of η. Another sum rule (called $S(\lambda_f \mu_f)$) is

$$\sum_{K_f,L_f} S_{(l)}^{(+)}\left(N;\ (\eta N,0)\ 0_{GS}^+ \to N+1;\ (\lambda_f \mu_f)K_f L_f\right) = |\ <\qquad >|^2$$

$$\times\ d\,(\lambda_f \mu_f)/d(\eta N,0),$$

where the triple barred matrix element $< ||| \ ||| >$ is the SU(3) CFP defined in (Devi and Kota 1991, 1992a) and $d(\lambda_\mu)$ is SU(3) dimension. We derived explicitly that $S(\lambda_f \mu_f) = N(1+\frac{3}{N})$ for $(\lambda_f \mu_f) = (4N + 4,0)$ and $3(1 + \frac{5}{4N})$ for $(4N, 2)$ irrep in SU_{sdg} (3) case. Similarly, in the SU_{sd} (3) × 1 g case $S(\lambda_f \mu_f)$ takes values $N(1 + \frac{3}{N})$ and $3(1 - \frac{1}{2N})$

for $(2N + 2,0)$ and $(2N - 2,2)$ irreps respectively. The expressions given in Figures 3, 4 satisfy both the above sum rules. The sum rules show that there is a one to one correspondence between the low-lying irreps of SU_{sdg} (3) and SU_{sd} (3) $\times$ 1 g limits and one difference between the two limits is in the nature of fragmentation of TNT strength. In data analysis, the sum rules can be used to distinguish between the SU_{sdg} (3) and SU_{sd} (3) $\times$ 1 g descriptions.